

## Article

# Experimental Study on a Solar Energy–Multi-Energy Complementary Heating System for Independent Dwellings in Southern Xinjiang

Jie Li <sup>1</sup>, Qian Yang <sup>1</sup>, Hong Chen <sup>1,2,\*</sup> and Sihui Huang <sup>1</sup>

<sup>1</sup> College of Water Resources and Construction Engineering, Shihezi University, Shihezi 832000, China; lijie\_shzu@shzu.edu.cn (J.L.); qianyang0077@163.com (Q.Y.); 18899121900@163.com (S.H.)

<sup>2</sup> School of Architecture, Huazhong University of Science and Technology, Wuhan 430074, China

\* Correspondence: chhwh@hust.edu.cn

**Abstract:** This study proposes a multi-energy complementary heating system that uses solar energy combined with biomass energy as the main heat source, with electricity as an auxiliary heat source. The system aims to tackle the low efficiency, high energy consumption, and pollution associated with traditional heating methods in rural southern Xinjiang, enhancing performance and productivity. It is designed to operate in five modes based on the region's climate and building heat load requirements. An experimental platform was set up in eight rural households in Tumushuk City, Xinjiang, where winter heating tests were conducted. The goal of this study was to analyze the economic and environmental benefits of the system. The results showed that the energy utilization efficiencies of the five modes were 56.84%, 74.34%, 70.1%, 63.13%, and 59.68%. The corresponding CO<sub>2</sub> emissions were 3.56 kg/d, 45.09 kg/d, 105.75 kg/d, 30.97 kg/d, and 76.79 kg/d. The environmental and economic costs for each mode were 0.0493 USD/d, 0.6398 USD/d, 1.5029 USD/d, 0.4384 USD/d, and 1.0905 USD/d. It is clear that as an auxiliary heat source, biomass energy is more beneficial than electricity. All five modes maintained indoor temperatures of 18 °C or higher, meeting winter heating needs in cold regions. The results of this study provide important data support for the promotion and application of solar and biomass heating systems in the rural areas of southern Xinjiang and also provide valuable references for solving the problem of decentralized heating in rural areas.

**Keywords:** solar energy; biomass energy; electricity; energy utilization efficiency; environmental benefits



Academic Editor: Federico Barrero

Received: 19 December 2024

Revised: 5 January 2025

Accepted: 9 January 2025

Published: 11 January 2025

**Citation:** Li, J.; Yang, Q.; Chen, H.; Huang, S. Experimental Study on a Solar Energy–Multi-Energy Complementary Heating System for Independent Dwellings in Southern Xinjiang. *Energies* **2025**, *18*, 298. <https://doi.org/10.3390/en18020298>

**Copyright:** © 2025 by the authors. Licensee MDPI, Basel, Switzerland. This article is an open access article distributed under the terms and conditions of the Creative Commons Attribution (CC BY) license (<https://creativecommons.org/licenses/by/4.0/>).

## 1. Introduction

According to the 2022 *Urban and Rural Construction Statistical Yearbook*, the construction area of rural residences in Xinjiang is 36,758.24 million square meters, with the area lacking centralized heating amounting to 36,340.85 million square meters, accounting for 98.8% of the existing rural residential area [1]. The traditional coal-fired-boiler heating model found in northern rural areas not only has low energy utilization efficiency but also causes severe environmental pollution [2,3]. This heating method not only fails to satisfy the thermal comfort requirements of residents but also significantly contributes to air pollution, thereby posing serious health and environmental concerns. This issue is particularly pronounced in the relatively underdeveloped southern Xinjiang region.

However, the southern Xinjiang region possesses significant resource advantages, including abundant solar energy resources, with an annual sunshine duration of 2685.3 h

and an annual total solar radiation of up to 1611.11 kWh/m<sup>2</sup>. Promoting the use of solar heating systems in this region could help alleviate fossil fuel consumption and reduce environmental pollution [4]. Nevertheless, due to the inherent limitations of solar energy, such as its intermittency [5] and variability [6], heating demands cannot be adequately met by relying solely on solar energy.

In southern Xinjiang, where agriculture and forestry are the main economic pillars, there are abundant biomass resources [7], particularly crop straw, which has an annual total output of approximately 18.9336 million tons [8]. This biomass can serve as a supplementary energy source to solar energy. Therefore, it is crucial to explore how to effectively integrate solar energy resources with biomass energy [9] to develop a multi-energy heating system suitable for the southern Xinjiang region and address the heating challenges faced by its residents [10,11].

Extensive research has been conducted on multi-energy heating systems, both in domestic and international contexts, with a focus on integrating clean energy sources, including solar energy, air source heat pumps, water source heat pumps, and biomass energy [12–16]. Gu Xianghong et al. [17] proposed a heating system that combines a solar wall with an air source heat pump featuring automatic control functions. They established a test platform and conducted research which demonstrated that under various weather conditions, the combined heating system can maintain indoor temperatures above 19 °C.

Ma Jiangyan et al. [18] proposed a composite heating system that integrates solar energy with air source and water source heat pumps, specifically designed for northern regions, utilizing TRNSYS for simulation studies. Their results indicated that the heating system achieves an average heating temperature of 60 °C and exhibits a strong adaptability to outdoor environments and heating terminals. Li et al. [11] developed a time-controlled heating system that utilizes a solar-assisted air source heat pump, built a test platform, and conducted tests. Their findings revealed that the combined heating system enhances thermal comfort in rooms while providing significant economic and environmental benefits.

Huang et al. [19] developed a heating system for a Beijing tech park, examining a reclaimed water heat pump's efficacy. Their findings revealed that this system excelled in providing warmth and slashed carbon emissions by over 62% compared to traditional gas boilers. Liu Yanfeng et al. [20] examined the solar–biomass energy combined heating resources in the northwest rural areas, concluding that the combined heating coverage rate in the Xinjiang Uyghur Autonomous Region could reach 96%.

Han Zhonghe and colleagues [21] established a rural distributed energy supply system based on solar and biomass energy. Their research showed that the system is well matched with the load of rural residential buildings, achieving an average primary energy utilization rate of 74%. This system can facilitate a reduction in coal combustion of 2.85 tons, as well as a decrease in emissions of 8.23 tons of CO<sub>2</sub>, and save costs amounting to 746.11 USD/year. Cui Haiting et al. [22] constructed a test platform to study the heating performance of a solar–biomass energy–valley–electricity–thermal–storage combined heating system. Their results indicated that the combined heating system can achieve an average indoor temperature of 19.76 °C, thereby meeting the heating requirements for cold regions during winter.

Our analysis of the existing literature indicates that most research on multi-energy complementary heating systems has concentrated on the performance and impacts of systems that integrate various clean energy sources, including solar energy, air source heat pumps, and biomass energy. However, there is relatively little research on the application of multi-energy heating systems in the southern Xinjiang region, and the lack of basic data hinders the promotion and implementation of these systems. Therefore, this study proposes a multi-energy complementary heating system, with solar energy and biomass energy as the main heat source and electrical energy as the backup heat source, aiming to

alleviate the dependence on traditional coal burning in Xinjiang during the heating period and to provide a reference for the promotion and utilization of solar energy and biomass energy in Xinjiang.

## 2. Introduction to the Experimental System

### 2.1. Test House Information

The test platform is situated in the rural area of the 8th Company in Tumxuk City, Xinjiang (latitude 39.97° N, longitude 79.09° E), classified as belonging to the cold climate zone A. The heating period lasts for 116 days, with a degree-day value of 2892 °C·d and an average annual minimum temperature of  $-7.3$  °C. The test house has a total construction area of 114.49 m<sup>2</sup>, as well as a story height of 3.0 m. It faces south and features a flat roof. Its exterior, along with a floor plan, are shown in Figure 1. The shape coefficient of the test house was calculated as  $S = F_o/V_o = 0.77$ , and details of the enveloping structure are provided in Table 1.

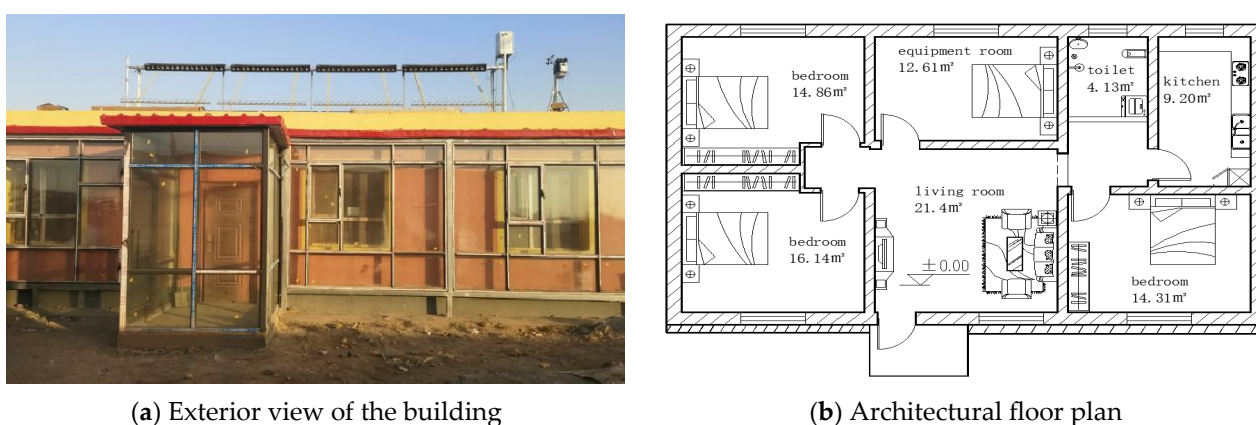


Figure 1. Building overview.

Table 1. Structural properties of the test enclosure.

Enclosure Structure	Construction Layers	Heat Transfer Coefficient W/(m <sup>2</sup> ·k)
Roof	Reinforced concrete (120 mm) + EPS insulation board (190 mm) + cement mortar (20 mm)	0.17
Wall	Fired perforated brick (370 mm) + EPS insulation board (120 mm) + cement mortar (20 mm)	0.23
Floor	Cement mortar (60 mm) + underfloor heating tubing + silver paper + EPS insulation board (120 mm) + fine aggregate concrete	0.48
Window	Double-cavity triple-seal (triple insulating glass 4 + 9A + 4 + 9A + 4) thermal break aluminum alloy window	1.8
Door	Insulated and sealed exterior door + thermal insulation foyer	1.5

### 2.2. Introduction to the Solar Energy–Multi-Energy Complementary Heating System

This study proposes a multi-energy complementary heating system that utilizes solar energy combined with biomass energy as the main heat source and electricity as an auxiliary heat source. The system is made up of five components (see Table 2 for details).

**Table 2.** Components of proposed multi-energy complementary heating system.

Components of the System	Detailed Composition
Solar part	The collector area is 24.37 m <sup>2</sup> , the angle of the solar collector is 50°, the volume of the hot water storage tank is 2 m <sup>3</sup> , and the plate heat exchanger is 0.6 m <sup>2</sup> .
Biomass fraction	The rated power of the biomass boiler is 15 kW, the fuel volume is 6 kg/h, and the manufacturer is Daqing Tingyu Technology Co., Ltd. (Daqing, China)
Electrical energy part	The electric auxiliary heater has a value of 7 kW.
Cryogenic radiant floor section	20 mm diameter underfloor heating coil with 150 mm intervals and five-way manifold.
Automatic control section	The control program, solenoid valve, temperature sensor, software and hardware, the heat meter meets the specification and is the model YNRC-DN25, and the circulating heat pump with 9 m head of 600 L/h is from Wilo.

Each component is interconnected by pipes, and the system equipment diagram is illustrated in Figure 2.

**Figure 2.** The MECH System equipment diagram.

The working principle of the heating system is as follows: the solar collector collects solar energy to heat the liquid-heat-exchange medium in the pipeline and then transports the hot water to the heating end through the heat pump to supply heat to the building. The pipe exchange medium on the collector side is composed of 55% ethylene glycol and 45% water, and its boiling point and freezing point are 107 °C and −40 °C, respectively, while the other pipeline exchange medium is water. When the outlet water temperature of the solar collector is  $\geq 5$  °C lower than the average temperature of the thermal storage tank, the heat collected by the solar collector is stored in the thermal storage tank through the plate heat exchanger, and when the average temperature of the thermal storage tank is  $\geq 35$  °C, the hot water in the thermal storage tank is then circulated through the low-temperature radiant floor system to heat the building. When solar energy is insufficient, the biomass boiler is activated to provide hot water for heating. If both solar and biomass energy sources are insufficient, the electric auxiliary heater will be activated to supply hot water for heating. A schematic diagram of the working principle of the heating system is shown in Figure 3.

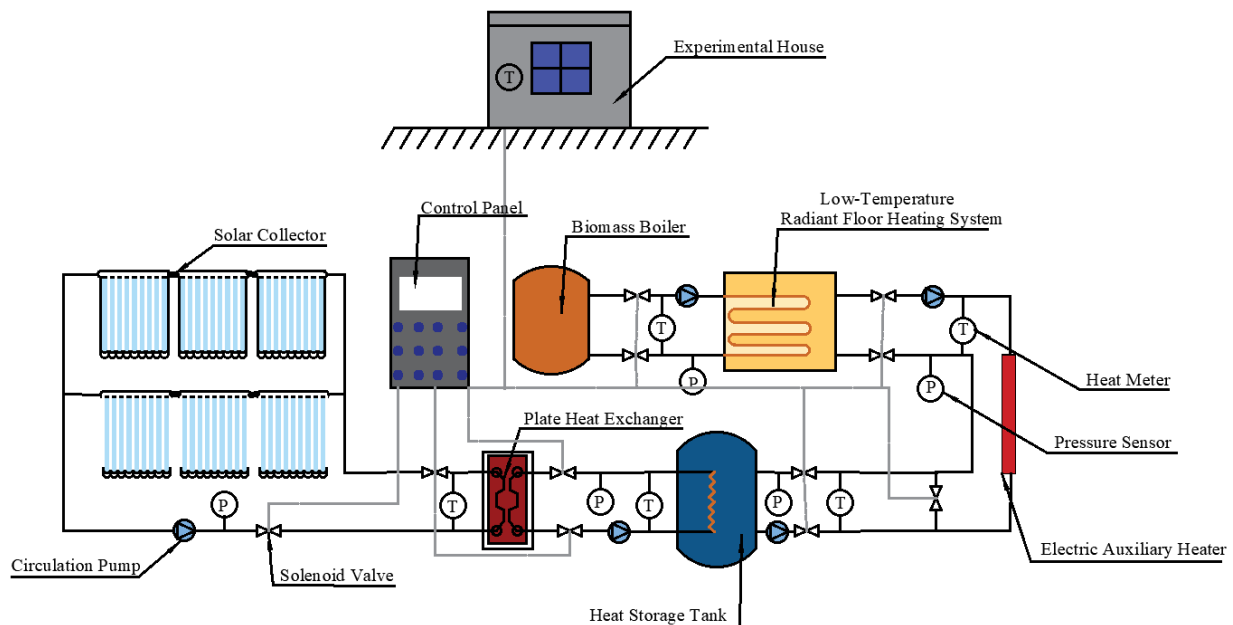


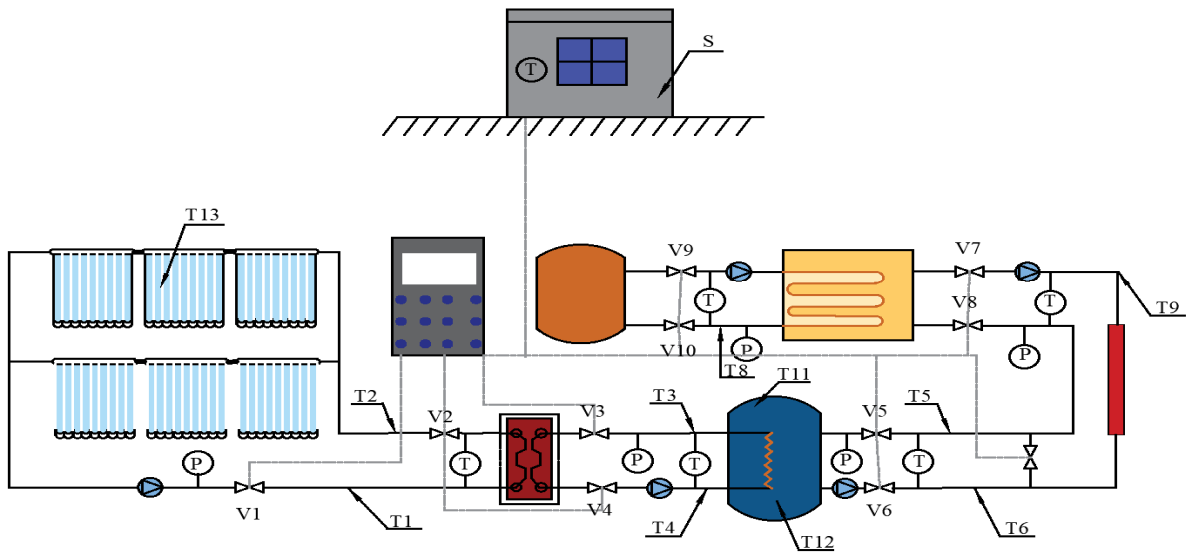
**Figure 3.** Working principle of the MECH system.

### 2.3. Test Content and Measurement Point Layout

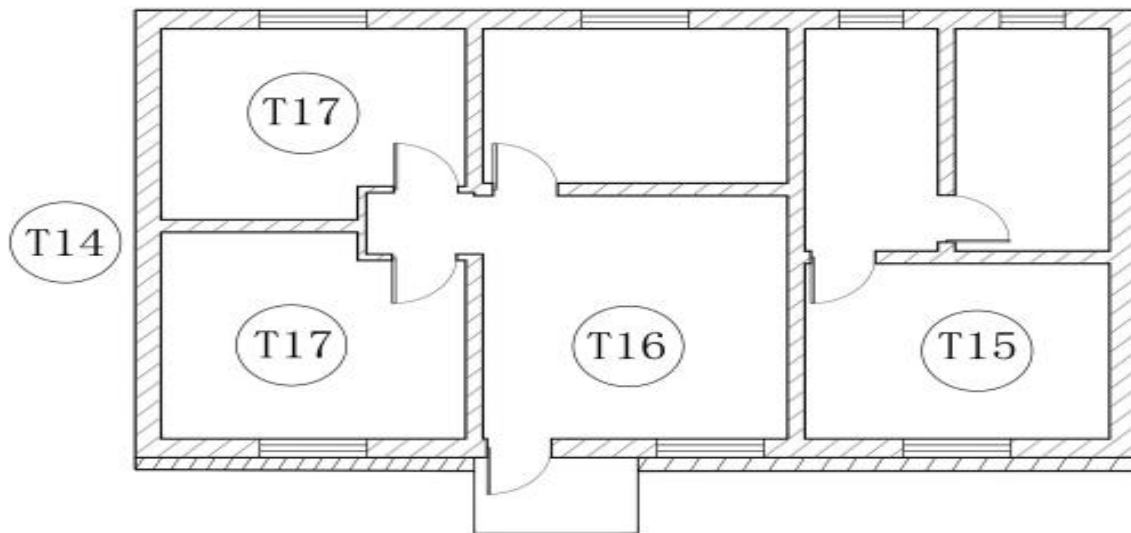
The winter heating test of the solar–multi-energy complementary heating system conducted in this study mainly included three parts, the outdoor meteorological parameters, the indoor environmental parameters, and the heating system parameters. Regarding the outdoor meteorological parameters, our research encompassed recording outside temperatures and the strength of sunlight exposure. Additionally, it encompassed indoor environmental parameters, specifically measurements of indoor temperature and relative humidity. In terms of the parameters of the heating system, we factored in the inlet and outlet water temperatures of the solar collector, thermal storage tank, biomass boiler, and electric auxiliary heater. Furthermore, we also measured the pipeline flow rate, circulation pump power, and the inlet and outlet water temperatures of the low-temperature radiant floor heating system, as well as the overall electricity consumption of the heating system. The layout of the measurement points is illustrated in Figure 4. During the test period, the pressure of the heat pump was measured using a pressure sensor, while the temperature and flow rate were monitored with thermal meters. Outdoor climate data were collected via a meteorological station. The system measurement instruments and parameters are detailed in Table 3. The test period spanned from 1 January to 12 January 2022, and from 11 March to 12 March 2022, totaling 14 days.

**Table 3.** Main parameters of the test instruments.

Testing Equipment	Specifications and Model	Project	Range	Error
Single-Temperature Data Logger	TR001	Temperature	−20–95 °C	±5%
Pressure Sensor	PT124G-111	Pressure	0–1.6 MPa	±1%
Heat Meter	YNRC-DN25	Temperature	0.07–7 m <sup>3</sup> /h	±5%
		Flow Rate	4–95 °C	±5%
Power Monitoring Device	LU-193	Electrical Energy	AC85~265 V	±0.5%
			DC85~330 V	
Weather Station	Vantage Pro2	Temperature	−40~65 °C	±5%
		Solar Radiation	0–1800 W/m <sup>2</sup>	±5%



(a) System measurement point layout diagram



(b) Room measurement point layout diagram

**Figure 4.** Layout of test points for the MECH system testing.

Figure 4a,b illustrate the measurement point layout for the multi-energy complementary heating system. T1 is the return water temperature at the solar flat plate heat exchanger; T2 is the supply water temperature at the solar flat plate heat exchanger; T3 is the supply water temperature at the plate heat exchanger thermal storage tank; T4 is the return water temperature at the plate heat exchanger thermal storage tank; T5 is the supply water temperature at the thermal storage tank floor heating; T6 is the return water temperature at the thermal storage tank floor heating; T7 is the return water temperature at the biomass boiler floor heating; T8 is the supply water temperature at the biomass floor heating; T9 is the return water temperature at the auxiliary electric heating floor heating; T10 is the supply water temperature at the auxiliary electric heating floor heating; T11 is the upper temperature of the thermal storage tank; T12 is the lower temperature of the thermal storage tank; T13 is the temperature of the solar collector panel; T14 is the outdoor temperature; T15 is the indoor temperature of room 1; T16 is the indoor temperature of room 2; T17 is the indoor temperature of room 3; T18 is the indoor temperature of room 4; P is the pipeline flow rate; and S is the solar irradiance.

#### 2.4. Operating Strategy of the Solar Energy Multi-Energy Complementary Heating System

Combined with the resource advantages of the south Xinjiang region, which is rich in solar energy and biomass energy, and based on the characteristics of common local raw materials such as cotton stalks and fruit tree branches, we optimize the crushing, drying, and molding processes to improve the fuel density and combustion stability, so as to increase the combustion efficiency of the biomass boiler and create a precedent for decentralized high-efficiency heat collection, which is in line with the demand for regional energy use. However, this heating system prioritizes the use of solar and biomass energy and due to the distance between the experimental house and the biomass fuel production facility, replenishing the biomass fuel within a short period of time may be challenging. Therefore, electricity is used as a supplementary energy source.

Using outdoor environmental parameters and indoor temperature as control benchmarks, and according to the temperatures listed in the “Design Standard for Energy Conservation of Residential Buildings in Severe Cold and Cold Areas” (JGJ26-2018) for which the human body experiences thermal balance and comfort, the most unfavorable indoor temperature thresholds are determined to be 18 °C and 22 °C. The multi-energy complementary heating system was designed with five operating modes:

Solar heating mode (Mode 1);

Biomass energy heating mode (Mode 2);

Electrical energy heating mode (Mode 3);

Solar energy combined with biomass energy heating mode (Mode 4);

Solar energy combined with electrical energy heating mode (Mode 5).

The remainder of this section details the specific operating strategies for each mode.

##### 2.4.1. Solar Heating Mode (Mode 1)

When the solar radiation is sufficient, meaning it can meet the building’s heating demands, the system operates in Mode 1. Specifically, if the outlet water temperature of the solar collector is 5 °C higher than the average temperature of the thermal storage tank, valves V1–V4 open to store heat in the thermal storage tank via the plate heat exchanger. When the average temperature of the thermal storage tank reaches or exceeds 35 °C, valves V5–V8 open to supply heat to the indoor space through the low-temperature radiant floor heating system. This system shuts down when the temperature in the least favorable room is  $\geq 22$  °C or when the thermal storage tank temperature drops to  $\leq 30$  °C. Additionally, if the outlet water temperature of the solar collector is  $\leq 1$  °C above the average temperature of the thermal storage tank, valves V1–V4 close, and solar heat collection stops.

##### 2.4.2. Biomass Energy Heating Mode (Mode 2)

When the outdoor climate experiences continuous overcast, rainy, or snowy conditions that make it impossible to utilize solar energy for heating, the system switches to Mode 2, with the specific operations as follows: when the temperature in the least favorable room is  $\leq 18$  °C, valves V9–V10 are opened to activate the biomass boiler, which heats the fluid in the pipeline for indoor heating. Conversely, when the temperature in the least favorable room reaches or exceeds 22 °C, valves V9–V10 are closed, and the biomass boiler ceases operation.

##### 2.4.3. Electrical Energy Heating Mode (Mode 3)

When the solar energy is insufficient for heating and there is a shortage of biomass fuel, the system switches to Mode 3, with the specific operations being as follows: when the temperature in the least favorable room is  $\leq 18$  °C, valves V7–V8 are opened to activate the electric auxiliary heater, which warms the fluid in the pipeline for indoor heating.

Conversely, when the temperature in the least favorable room reaches or exceeds 22 °C, valves V7–V8 are closed, and the electric auxiliary heater ceases operation.

#### 2.4.4. Solar Energy Combined with Biomass Energy Heating Mode (Mode 4)

When solar energy cannot provide sufficient heat to the indoor space, the system switches to Mode 4, activating the biomass boiler for auxiliary heating. The specific operations are as follows: when the average temperature of the thermal storage tank is  $\leq 30$  °C and the temperature in the least favorable room is  $\leq 18$  °C, valves V9–V10 are opened to activate the biomass boiler, which heats the fluid in the pipeline for indoor heating. When the temperature in the least favorable room reaches or exceeds 22 °C, valves V9–V10 are closed, the biomass boiler shuts down, and indoor heating ceases. If the temperature in the coolest room is  $\leq 22$  °C and the thermal storage tank averages a value of  $\geq 35$  °C, valves V5–V8 open, activating solar energy mode. Should the temperature in the least favorable room still be  $\leq 22$  °C while the thermal storage tank falls to  $\leq 30$  °C, valves V9 and V10 reopen, reactivating the biomass boiler, which provides heat until the least favorable room reaches  $\geq 22$  °C. At that point, valves V5–V10 are closed, and indoor heating is halted.

#### 2.4.5. Solar Energy Combined with Electrical Energy Heating Mode (Mode 5)

When solar energy cannot provide sufficient heat to the indoor space and there is no biomass fuel available, the system switches to Mode 5, activating the electric auxiliary heater for heating. The specific operations are as follows: when the solar and biomass sections are unable to provide enough heat to the indoor space—specifically, when the average temperature of the thermal storage tank is  $\leq 30$  °C and the temperature in the least favorable room is  $\leq 18$  °C—valves V7–V8 are opened to activate the electric auxiliary heater, which warms the fluid in the pipeline for indoor heating. When the temperature in the least favorable room reaches or exceeds 22 °C, valves V7–V8 are closed, the electric auxiliary heater is turned off, and indoor heating is stopped. If the temperature in the coolest room is  $\leq 22$  °C and the thermal storage tank averages a value of  $\geq 35$  °C, valves V5–V8 open, activating solar energy mode. Should the temperature in the least favorable room still be  $\leq 22$  °C while the thermal storage tank falls to  $\leq 30$  °C, valves V7 and V8 reopen, reactivating the electric auxiliary heater for heating until the least favorable room reaches  $\geq 22$  °C. At that point, valves V5–V10 are closed, and indoor heating is halted.

### 3. Results

#### 3.1. Solar Heating Mode (Mode 1) Result

When solar energy provides sufficient heat to meet the thermal demands of the building, the system operates in Mode 1. The test period for this mode was from March 1 to 2, 2022. The outdoor meteorological parameters and the details of the system operation are presented in Figure 5.

Figure 5 shows that during Mode 1 operation, the outdoor average temperature was 6.25 °C, with a peak solar irradiance of 678 W/m<sup>2</sup> and an average of 467 W/m<sup>2</sup>. The indoor temperature ranged from 18 °C to 23.16 °C, with an average of 20.15 °C.

On March 1, during system operation, the indoor temperature dropped to 18 °C at 6:16 A.M., prompting the thermal storage tank to begin supplying heat, while the average temperature of the thermal storage tank started to decrease. By 10:30 A.M., with sufficient solar radiation, the solar heating system began to collect heat. After a brief decrease, the temperature of the thermal storage tank began to rise slowly at 12:00 P.M., during which time the thermal storage tank continued to supply heat to the indoor space. At 2:00 P.M., the indoor temperature reached 22 °C, at which point heating was stopped, although the solar

collector continued to collect heat. By 8:00 P.M., solar radiation was no longer sufficient for heat collection, and the solar collector ceased operation. The solar collector and thermal storage tank operated for 7.89 h and 9.5 h, respectively. The operation pattern on March 2 was largely consistent with that of the previous day, with the solar heating and thermal supply operating for 9.5 h and 7.0 h, respectively. During the operation of Mode 1, the solar heat supply amounted to 98.27 kW·h, while the power consumption of the system’s circulation pump and automatic control system was 4.985 kW·h.

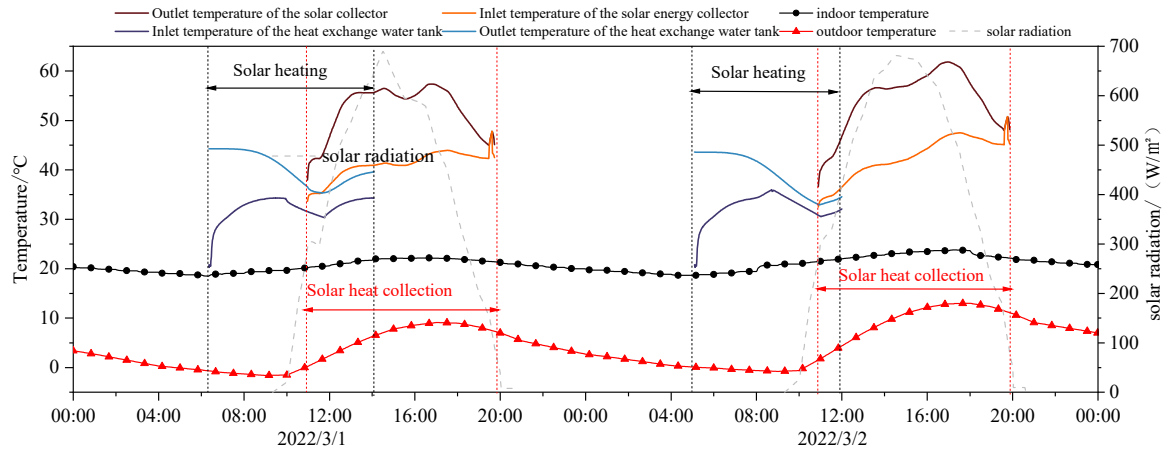


Figure 5. Test data of the MECH system operating in Mode 1.

### 3.2. Biomass Heating Mode (Mode 2) Result

When the outdoor climate is characterized by continuous overcast, rainy, or snowy conditions that make it impossible to utilize solar energy for heating, the system switches to Mode 2. The test operation period for this mode was from 1 January to 2 January 2022. Figure 6 illustrates the outdoor climatic conditions and the details of the system operation.

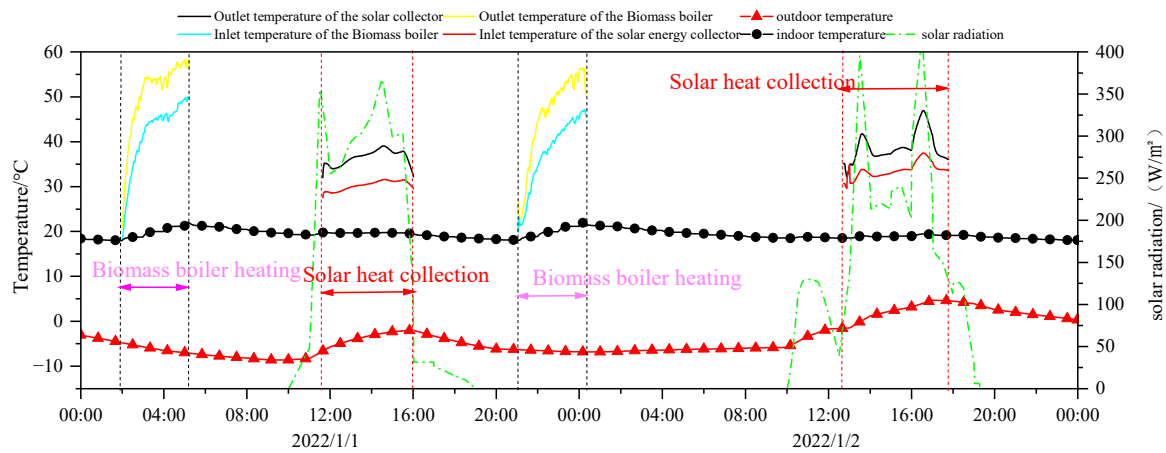


Figure 6. Test data of the MECH system operating in Mode 2.

Figure 6 shows that during Mode 2 operation, the outdoor average temperature was  $-3.19\text{ }^{\circ}\text{C}$ , with a peak solar irradiance of  $382.35\text{ W/m}^2$  and an average of  $172.68\text{ W/m}^2$ . The indoor temperature ranged from  $18\text{ }^{\circ}\text{C}$  to  $22\text{ }^{\circ}\text{C}$ , with an average of  $19.37\text{ }^{\circ}\text{C}$ .

In the early morning of 1 January, at 2:00 A.M., the room temperature dropped to  $18\text{ }^{\circ}\text{C}$ . Since the thermal storage tank temperature did not reach  $35\text{ }^{\circ}\text{C}$ , it was insufficient to provide heat for the room; therefore, the biomass boiler was activated to heat the space. At 5:14 A.M., the building temperature reached  $22\text{ }^{\circ}\text{C}$ , prompting the biomass boiler to cease operation, after which the room temperature began to slowly decline. At 11:39 A.M., the

solar irradiance met the conditions for heat collection, and solar heat collection commenced, allowing the thermal storage tank to start accumulating heat. By 4:00 P.M., when solar radiation became insufficient, the thermal storage tank stopped accumulating heat, at which point its temperature was 34.58 °C. At 9:00 P.M., the indoor temperature dropped to 18 °C. As the heat collected from solar energy did not raise the temperature of the thermal storage tank to a sufficient level for heating, the biomass boiler was responsible for heating the room. At 12:19 A.M. on 2 January, the room temperature reached 22 °C, leading to the shutdown of the biomass boiler and the cessation of heating. During Mode 2 operation, the solar collector only performed heat collection without providing heating, and all room heat requirements were met by the biomass boiler. The solar collector operated for 9.35 h and the biomass boiler operated for 6.52 h, 24.05 kg of biomass fuel was consumed and the power consumption of the system's circulation pump and automatic control system was 8.35 kW·h.

### 3.3. Electrical Auxiliary Heating Mode (Mode 3) Result

Mode 3 serves as a supplement to Mode 2 and is activated when solar energy is unavailable for heating and there is a shortage of biomass fuel. The test operation period for this mode was from 4 January to 5 January 2022. The outdoor climatic conditions and the details of the system operation are illustrated in Figure 7.

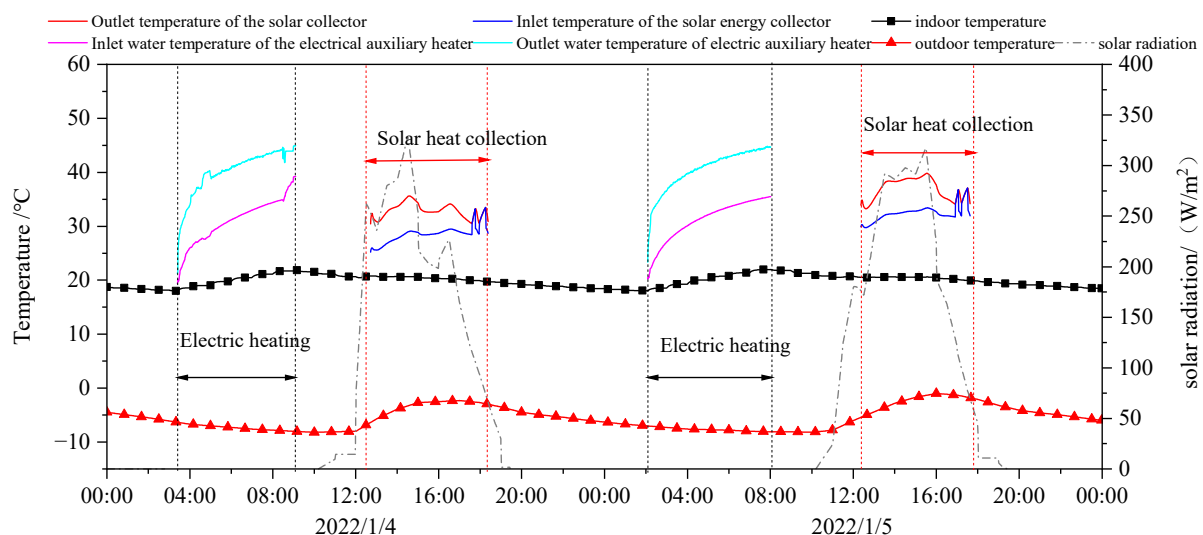


**Figure 7.** Test data of the MECH system operating in Mode 3.

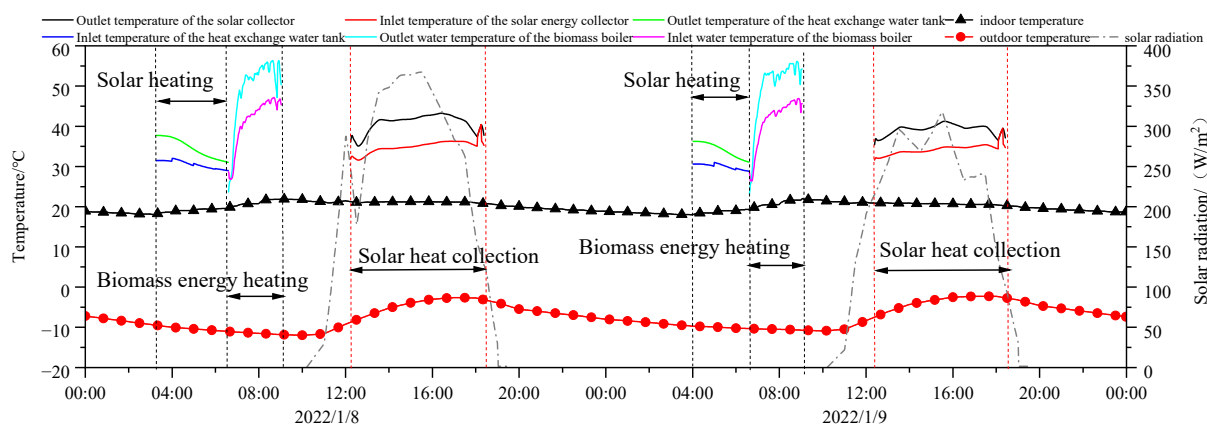
In Mode 3, as depicted in Figure 7, the average external temperature was  $-5.65$  °C. The incoming solar radiation reached a maximum of  $327.35$   $W/m^2$ , while the mean was  $151.82$   $W/m^2$ . Inside, temperatures varied between  $18$  °C and  $22$  °C, settling at an average of  $19.89$  °C.

In the early morning of 4 January, at 3:24 A.M., the room temperature dropped to  $18$  °C, prompting the electric auxiliary heater to be turned on to heat the room. By 9:06 A.M., the room temperature reached  $22$  °C, at which point the electric auxiliary heater was turned off, and the room temperature began to slowly decrease. At 12:43 P.M., the solar irradiance met the conditions for heat collection, and the solar heating system was activated, allowing the thermal storage tank to start accumulating heat. However, at 6:23 P.M., due to insufficient solar radiation, the thermal storage tank stopped accumulating heat. On 5 January, at 2:06 A.M., the indoor temperature dropped to  $18$  °C again. Since the thermal storage tank temperature did not reach the required heating temperature and there was a shortage of biomass fuel, the electric auxiliary heater was turned on once more for heating.

By 8:05 A.M. on 5 January, the room temperature reached 22 °C, and the electric auxiliary heater was shut off. During the test period, the electric auxiliary heater operated for 11.7 h for heating, while the solar collector operated for 10.38 h for heat collection. The electricity consumption of the electric auxiliary heater was 140.4 kW·h, and the power consumption of the system's circulation pump and automatic control system was 8.12 kW·h.

### 3.4. Solar Energy Combined with Biomass Energy Heating Mode (Mode 4) Result

When the solar energy cannot fully meet the thermal load of the building, the system switches to Mode 4. The test operation period for this mode was from 8 January to 9 January 2022. The outdoor climatic conditions and the system operation details are illustrated in Figure 8.



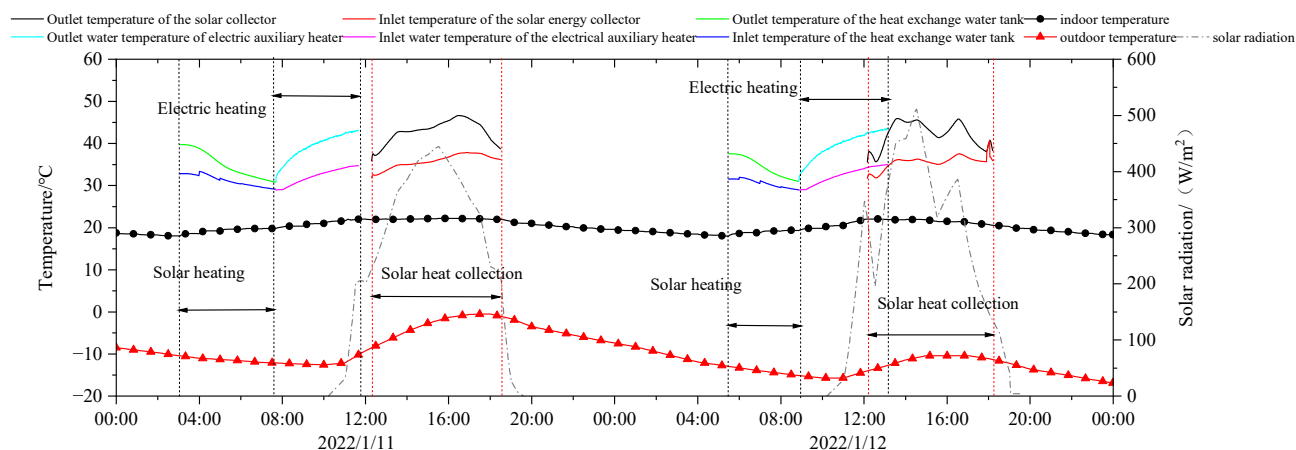
**Figure 8.** Test data of the MECH system operating in Mode 4.

Figure 8 shows that during Mode 4 operation, the outdoor average temperature was  $-7.45$  °C, with a peak solar irradiance of  $363.76$  W/m<sup>2</sup> and an average of  $225.37$  W/m<sup>2</sup>. The indoor temperature ranged from 18 °C to 22 °C, with an average of 20.02 °C.

In the early morning of 8 January, at 3:16 A.M., the room temperature dropped to 18 °C. At this time, the thermal storage tank temperature was 36.75 °C, which met the heating conditions, allowing the room to be heated using the heat provided by the thermal storage tank. By 6:35 A.M., the room temperature had risen to 19.55 °C, but the thermal storage tank temperature had dropped to 30 °C, no longer meeting the heating conditions. At this point, the system shut off solar heating and activated the biomass boiler, causing the room temperature to slowly rise again. By 9:02 A.M., the room temperature reached 22 °C, and the biomass boiler was shut off. At 12:14 P.M., the solar irradiance met the conditions for heat collection, and the solar collector began to collect heat, allowing the thermal storage tank to start accumulating heat. However, at 6:40 P.M., due to insufficient solar radiation, the solar collector stopped collecting heat and the thermal storage tank stopped accumulating heat. On 9 January, the system operation was similar to that of January 8. During the test period, the biomass boiler operated for heating for 5.9 h, while solar heating and heat collection occurred for 5.02 h and 12.41 h, respectively. The system consumed 19.02 kg of biomass fuel, and the circulation pump consumed 7.31 kW·h of electricity.

### 3.5. Solar Energy Combined with Electrical Energy Heating Mode (Mode 5) Result

Mode 5 complements Mode 4 and is activated when solar energy cannot provide sufficient heat to the indoor space and there is no biomass fuel available. The test operation period for this mode was from 11 January to 12 January 2022. The outdoor climatic conditions and the system operation details are illustrated in Figure 9.



**Figure 9.** Test data of the MECH system operating in Mode 5.

Figure 9 shows that during Mode 5 operation, the outdoor average temperature was  $-10.11\text{ }^{\circ}\text{C}$ , with a peak solar irradiance of  $512.35\text{ W/m}^2$  and an average of  $264.20\text{ W/m}^2$ . The indoor average temperature was  $20.2\text{ }^{\circ}\text{C}$ , fluctuating between  $18\text{ }^{\circ}\text{C}$  and  $22\text{ }^{\circ}\text{C}$ .

In the early morning of 11 January, at 3:04 A.M., the room temperature dropped to  $18\text{ }^{\circ}\text{C}$ . At this time, the thermal storage tank temperature was  $38.8\text{ }^{\circ}\text{C}$ , which met the heating conditions, prompting the system to activate the solar heating mode. By 7:40 A.M., the room temperature had risen to  $20.01\text{ }^{\circ}\text{C}$ , but the thermal storage tank temperature had dropped to  $30\text{ }^{\circ}\text{C}$ , no longer meeting the heating conditions. Consequently, the solar heating mode was turned off, and the electric auxiliary heater was activated, causing the room temperature to rise slowly again. At 11:44 A.M., the room temperature reached  $22\text{ }^{\circ}\text{C}$ , and the electric auxiliary heater ceased operation. At 12:14 P.M., the solar irradiance met the conditions for heat collection, and the solar collector began to collect heat, allowing the thermal storage tank to start accumulating heat. However, at 6:30 P.M., due to insufficient solar radiation, the thermal storage tank stopped accumulating heat. On January 12, the system operation was similar to that on January 11. During the test period, electric auxiliary heating, solar heating, and heat collection occurred for 8.3 h, 8 h, and 12.46 h, respectively. The electricity consumption of the electric auxiliary heater was  $99.6\text{ kW}\cdot\text{h}$ , and the power consumption of the system's circulation pump was  $8.25\text{ kW}\cdot\text{h}$ .

### 3.6. Results Analysis

This study analyzed experimental data to assess equipment operation time and power consumption across five operating modes. The findings show that the system efficiently meets the building's thermal load when solar energy is plentiful. However, when solar energy is limited, the system leverages biomass or electrical energy as supplementary heat sources to optimize energy usage and meet thermal load demands.

## 4. Discussion of System Performance and Benefit Analysis

### 4.1. System Performance Analysis

To investigate the operational characteristics of the multi-energy complementary heating system under different modes, a quantitative analysis was conducted on the system's heating power, energy utilization rate, and solar guarantee rate.

The energy utilization rate and solar guarantee rate of the multi-energy complementary heating system are calculated using the following formulas:

$$\eta = \frac{Q_{\alpha}}{W_c} \quad (1)$$

$$Q_{\alpha} = Q_s + Q_b + Q_e \quad (2)$$

$$W_c = W_b + W_p + W_e + W_a \quad (3)$$

In the above formulas  $\eta$  represents the energy utilization rate;  $Q_{\alpha}$  is the system's heat supply, in kW·h;  $W_c$  is the system's energy consumption, in kW·h;  $Q_s$  is the heat supply from the collector;  $Q_b$  is the heat supply from the biomass boiler;  $Q_e$  is the heat supply from the electric auxiliary heater;  $W_b$  is the consumption of biomass fuel;  $W_p$  is the electricity consumption of the system's circulation pump;  $W_e$  is the electricity consumption of the electric auxiliary heater; and  $W_a$  is the electricity consumption of the automatic control system.

$Q_s$ ,  $Q_b$ , and  $Q_e$  can be calculated according to the following formula [23]:

$$Q_i = \int q(t)dt = \int mC_p[T_{out}(t) - T_{in}(t)]dt \quad (4)$$

In this formula  $i$  represents  $s$ ,  $b$ , and  $e$ ;  $t$  represents time;  $q(t)$  is the heat supply power of the system, in kW;  $C_p$  is the specific heat capacity of the fluid medium, in J/kg·°C;  $T_{out}$  is the outlet medium temperature, in °C; and  $T_{in}$  is the inlet medium temperature, in °C.

The solar guarantee rate of the multi-energy complementary heating system is calculated according to the following formula [24]:

$$SF = \frac{Q_s}{Q_h} \quad (5)$$

In the above formula,  $SF$  represents the solar guarantee rate, and  $Q_h$  is the building heat load, in kW.

Based on the aforementioned formulas, specifically (1) to (4), the heat supply power, energy utilization rate, and solar guarantee rate for the system's five modes were calculated. Figure 10 shows the heating power of the three heating modes in the five different operation modes. The average power of solar heating is 6.45 kW, the average power of biomass heating is 11.23 kW, and the average power of electric auxiliary heating is 7.95 kW. Compared with the efficiency of these heating methods, the biomass heating efficiency is the highest. This is because the biomass boiler has a high combustion efficiency and a fast-heating speed, which means it can effectively convert the energy in the biomass fuel into heat energy during the energy conversion process. In contrast, solar heating is the least efficient. In solar heating mode, the inlet and return water temperature is lower, and during the heating process, the temperature difference between the inlet and return water gradually decreases. This means that the amount of heat that a solar heating system can transfer gradually decreases during heat transfer, resulting in limited heating efficiency. Of particular noteworthiness is that when analyzing the thermal efficiency of the solar collector in different modes, it was found that the solar collector in Mode 1 reached 9.58 kW, which was significantly higher than that of the other four modes. The main reason for this phenomenon is that the external environment in which Mode 1 is located is ideal. When Mode 1 is in play, the outside temperature is higher, and this warmer environment helps to reduce heat loss during heat collection and transfer in the solar collector. At the same time, the high intensity of solar radiation during Mode 1 operation means that the solar collector is able to receive more solar radiation energy, which, in turn, means that this energy is converted into heat more efficiently so that the solar collector in Mode 1 can achieve high thermal collection efficiency.

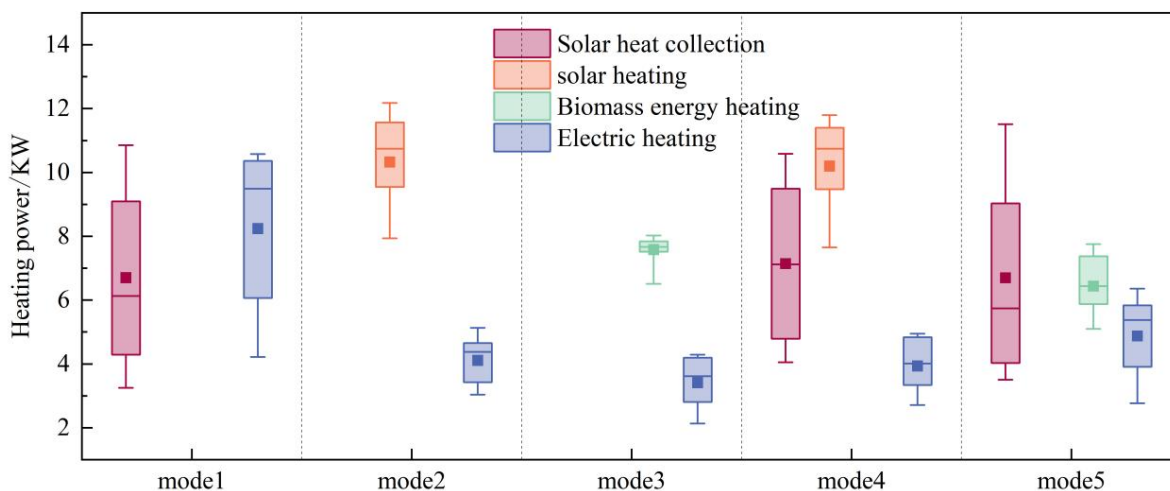


**Figure 10.** Heating power in different modes of MECH systems.

Table 4 presents the energy utilization rates of the system in different modes, with Mode 1 exhibiting the lowest rate. This is due to the relatively low inlet and outlet water temperatures during solar heating, leading to increased losses in the heating process. Significant heat losses also occur in the plate heat exchanger and the outdoor pipelines during heat collection from the solar collector.

**Table 4.** Energy utilization rate under different models of multi-clean-energy complementary heating systems.

Operating Mode	Type	Solar Energy/kW·h	Biomass Energy/kW·h	Electrical Energy/kW·h	Energy Utilization Efficiency/%
Mode 1	Heat Supply	98.72			56.84
	Consumption	166.70		4.98	
Mode 2	Heat Supply		89.28		74.34
	Consumption		111.86	8.35	
Mode 3	Heat Supply		105.95		70.10
	Consumption			148.40	
Mode 4	Heat Supply	28.26	66.45		63.13
	Consumption	54.39	88.50	7.13	
Mode 5	Heat Supply	35.77		69.83	59.68
	Consumption	69.09		107.80	

Note: “Consumption” refers to the amount of solar energy collected by the solar collectors during the test period, while “Heat Supply” refers to the amount of heat provided by the thermal storage tank to the building.

Furthermore, the energy utilization rate of the system under the auxiliary heat source heating mode is higher than that under the solar-coupled auxiliary heat source heating mode. This is because when solar energy is involved in heating, the system’s heat losses increase, leading to a decrease in the energy utilization rate.

Table 5 shows the solar guarantee rate of the system in different modes. The solar guarantee rates for Modes 4 and 5 are approximately 46% and 38%, respectively, with the contribution rate of solar energy not exceeding 50%. This is attributed to the low outdoor ambient temperature and the significant building heat load, which necessitate the use of auxiliary heat sources in cold regions. Therefore, considering the comprehensive test operation of Modes 2–5 from the perspective of energy utilization rate, biomass energy should be prioritized when selecting auxiliary heat sources.

**Table 5.** Solar energy guarantee rate.

Operation Mode	Solar energy Guarantee Rate (%)
Mode 1	100
Mode 4	46.10
Mode 5	36.57

#### 4.2. Analysis of the System's Environmental Benefits

The environmental impact of the multi-energy complementary heating system can be calculated according to the following formula [25]:

$$X_{CO_2} = Y_{CO_2} W_{energy} t_{working} \quad (6)$$

$$C_{co_2} = X_{co_2} c_{co_2} \quad (7)$$

In the above formula  $X_{CO_2}$  represents the  $CO_2$  emission during the system's operation, in  $kg-CO_2/h$ , and  $Y_{CO_2}$  represents the  $CO_2$  emission value of the system's heat source, in  $kg-CO_2/kW \cdot h$ . In this study, the  $CO_2$  emission factor for biomass pellet fuel was  $0.35 kg-CO_2/kW \cdot h$  [26], and the  $CO_2$  emission factor for electricity was  $0.712 kg-CO_2/kW \cdot h$  [16].  $W_{energy}$  represents the power of the system's heat source, in  $kW$ ;  $t_{energy}$  represents the working time of the system, in  $h$ ;  $C_{co_2}$  represents the environmental economic cost, in  $USD$ ; and  $C_{co_2}$  represents the international carbon price,  $0.0142 USD/kg-CO_2$ .

To understand the environmental impact of the system under different modes, an assessment of  $CO_2$  emissions and environmental economic costs was conducted for each system mode. Table 6 presents the  $CO_2$  emissions, system working time, and environmental economic costs for heating Modes 1–5.

**Table 6.**  $CO_2$  emissions and environmental economic costs of the multi-clean-energy complementary heating system.

Operating Mode	System Operating Time			$CO_2$ Emissions (kg/d)	Environmental Economic Cost (USD/d)
	Circulation Pump	Biomass Boiler	Electric Auxiliary Heater		
Mode 1	28.84			3.56	0.0493
Mode 2	15.6	6.52		45.09	0.6398
Mode 3	22.08		11.7	105.75	1.5029
Mode 4	23.33	5.9		30.97	0.4384
Mode 5	28.76		8.3	76.79	1.0905

It can be observed that Mode 1 has the lowest  $CO_2$  emissions and environmental economic costs. Modes 3 and 5, which utilize electricity as an auxiliary heat source, exhibit the highest  $CO_2$  emissions and economic costs, followed by Modes 2 and 4, which use biomass energy as an auxiliary heat source. Compared to Mode 3, Mode 2 reduces  $CO_2$  emissions by  $60.66 kg/d$  and the environmental economic cost by  $0.8631 USD/d$ . Similarly, compared to Mode 5, Mode 4 reduces  $CO_2$  emissions by  $45.82 kg/d$  and the environmental economic cost by  $0.6521 USD/d$ .

Therefore, from an energy perspective, biomass energy should be prioritized as an auxiliary heat source.

## 5. Conclusions

The study introduces a hybrid heating system designed to meet the heating demands of rural homes in colder areas, utilizing a mix of solar power, biomass, and electricity.

Five operational modes were designed to select an appropriate heating method based on different environmental conditions and states, thereby enhancing the system's flexibility and adaptability. We scrutinized the system's energy efficiency, alongside its environmental and fiscal advantages, via empirical data examination. This investigation lays the groundwork for adopting integrated multi-energy heating systems in homes across southern Xinjiang. Key takeaways from this inquiry are outlined below:

- (1) When solar energy is abundant and Mode 1 is being used for room heating, the system provides 98.72 kW·h of heat to the building, effectively meeting its thermal load. During Mode 1 operation, the system's electricity consumption is only 4.98 kW·h, resulting in an energy utilization rate of 56.84%.
- (2) When the solar energy collected by the system is not enough to initiate Mode 1, Modes 2 or 3 are employed for room heating. Modes 2 and 3 provide 89.28 kW·h and 105.95 kW·h of heat, respectively, with system energy utilization rates of 74.34% and 70.10%, respectively, indicating that Mode 2 is slightly more efficient than Mode 3. However, during operation, Mode 3's CO<sub>2</sub> emissions are 60.66 kg/d higher than those of Mode 2, and the environmental economic cost is 0.8631 USD/d higher.
- (3) When the solar energy collected by the system is insufficient to support room heating alone, Mode 4 or 5 are activated. Mode 4 provides 94.71 kW·h of heat to the room, with solar energy and biomass energy contributing 28.26 kW·h and 66.45 kW·h, respectively. In contrast, Mode 5 provides 105.6 kW·h of heat to the room, with solar energy and electrical energy contributing 35.77 kW·h and 69.83 kW·h, respectively. The system's energy utilization rates under the two modes are 63.13% and 59.86%, respectively. During operation, the system's CO<sub>2</sub> emissions for Mode 5 are 45.82 kg/d higher than those for Mode 4, and the environmental economic cost increases by 0.6521 USD/d.
- (4) The proposed system supports five heating modes, ensuring that the indoor temperature in the test room remains above 18 °C, meeting the heating demands of colder regions during winter. Given the energy efficiency and advantages of the system, biomass energy emerges as a particularly appropriate supplementary source for this multi-energy complementary heating system. However, in extreme cases where biomass fuel cannot be replenished in time, the system should be equipped with an electric auxiliary heater as a backup heating device.

**Author Contributions:** Data curation, Q.Y.; formal analysis, S.H.; methodology, H.C.; software, J.L.; visualization, S.H.; writing—original draft, J.L. All authors have read and agreed to the published version of the manuscript.

**Funding:** This research was funded by the Xinjiang Production and Construction Corps Shihezi City Science and Technology Innovation Program via grant number 2024GY05.

**Data Availability Statement:** Data will be made available on request.

**Conflicts of Interest:** The authors declare no conflicts of interest.

## References

1. National Bureau of Statistics of the People's Republic of China. *China Statistical Yearbook*; China Statistics Press: Beijing, China, 2022.
2. Wang, Q. Optimization Study of Electric Boiler Coupled with Air Source Heat Pump Thermal Energy Storage Heating System in Xinjiang Region. Ph.D. Thesis, Qingdao University of Technology, Qingdao, China, 2023. [[CrossRef](#)]
3. Yang, B.; Qi, Y.; Hou, Y. Performance Study of Solar + Biomass Heating Systems in Northern Rural Buildings. *Build. Energy Effic.* **2023**, *51*, 109–117.
4. Gao, Q.; Zhou, L.; Zhang, H.; Wang, Y.; Wu, P. Research on the Distribution and Utilization of Agricultural and Forestry Biomass Resources in Southern Xinjiang. *Xinjiang Agric. Mech.* **2021**, *1*, 17–22. [[CrossRef](#)]

5. Gu, W.; Gulipar, Y.H.; Jiang, L.; Zang, X. Research on the Spatial and Temporal Distribution Characteristics and Zoning of Solar Energy Resources in Southern Xinjiang. *Arid. Land Geogr.* **2021**, *44*, 1665–1675.
6. Yu, H.; Zhang, Y.; Zhang, Q.; Li, G.; Yan, H. Research on the System Construction of Supplier Evaluation and Selection for the Solar Thermal Application Industry. *Acta Energetica Solaris Sin.* **2020**, *41*, 305–309.
7. Pompelli, M.F.; Jarma Orozco, A.D.J.; De Oliveira, M.T.; Monteiro, R.; Bruno, R.; Barbosa, M.O.; Guida Santos, M.; Morais de Oliveira, A.F.; de Almeida-Cortez, J.S. The Global Energy Crisis and Brazil's Role in the Issue of Biofuels. *Agron. Colomb.* **2011**, *29*, 423–433.
8. Gao, Q. The Status Quo of Biomass Resources Utilization in Southern Xinjiang and Detection of Biomass Characteristics of Fruit Tree Branches. Ph.D. Thesis, Tarim University, Alar, China, 2021. [\[CrossRef\]](#)
9. Xu, J.; Gao, Y. Application of Biomass Power Generation Technology in Rural Electricity. *Rural. Sci. Exp.* **2024**, *19*, 45–47.
10. Cao, C.; Liu, L.; Quan, C.; Rui, Z. Research on the Application of Multi-Energy Complementary Heating System in Civil Buildings in Severe Cold Regions. *Qinghai Sci. Technol.* **2022**, *29*, 187–192.
11. Li, G.; Dai, L.; Bai, J.; Li, X.; Lu, J. Research Progress and Prospect of Multi-Energy Complementary Heat Pump System. *Energy Energy Conserv.* **2022**, *7*, 24–26+50. [\[CrossRef\]](#)
12. Bor, D.M.V.D.; Ferreira, C.A.I.; Kiss, A.A. Low Grade Waste Heat Recovery Using Heat Pumps and Power Cycles. *Energy* **2015**, *89*, 864–873.
13. Sun, F.; Cheng, L.; Fu, L.; Gao, J. New Low Temperature Industrial Waste Heat District Heating System Based on Natural Gas Fired Boilers with Absorption Heat Exchangers. *Appl. Therm. Eng.* **2017**, *125*, 1437–1445. [\[CrossRef\]](#)
14. Zhang, X.; Yang, J.; Fan, Y.; Zhao, X.; Yan, R.; Zhao, J.; Myers, S. Experimental and Analytic Study of a Hybrid Solar/Biomass Rural Heating System. *Energy* **2020**, *190*, 116392. [\[CrossRef\]](#)
15. Mirosław, Z.; Grzegorz, W. Estimation of Energy Savings Resulting from the Cooperation of an Air to Water Heat Pump with a Solar Air Heater. *Sol. Energy* **2023**, *250*, 182–193.
16. Zhao, M.; Gu, Z.L.; Kang, W.B.; Liu, X.; Zhang, L.Y.; Jin, L.W.; Zhang, Q.L. Experimental Investigation and Feasibility Analysis on a Capillary Radiant Heating System Based on Solar and Air Source Heat Pump Dual Heat Source. *Appl. Energy* **2016**, *185*, 2094–2105. [\[CrossRef\]](#)
17. Gu, X.; Peng, Q.; Chen, L.; Gao, J. Experimental and Simulation Research on Solar Wall-Air Source Heat Pump Combined Heating System. *Build. Sci.* **2021**, *37*, 61–66+136. [\[CrossRef\]](#)
18. Ma, J.; Deng, B.; Hou, W.; Nan, S.; Zhou, Y.; Wang, D.; Liu, Y. Performance Analysis of a Solar Energy Coupled Air-Source and Water-Source Heat Pump Composite Heating System. *HVAC* **2023**, *53*, 22–27. [\[CrossRef\]](#)
19. Huang, C.; Wei, W.; Sun, Y.; Wang, W.; Li, Z.; Wang, S.; Deng, S. Energy Saving and Peak Load Shifting Performance of Tail Water Source Heat Pump Integrated with Large-Scale Thermal Storage Pool Space Heating System in Technology Park. *Energy Convers. Manag.* **2023**, *287*, 117032. [\[CrossRef\]](#)
20. Liu, Y.; Wang, M.; Wang, D.; Zhou, Y. Feasibility Analysis of Solar Energy and Biomass Energy Combined Heating Resources in Northwest China Rural Area. *Acta Energetica Solaris Sin.* **2018**, *39*, 1045–1051.
21. Han, Z.; Qi, C.; Ding, J.; Liu, M.; Wang, S. Research on Rural Distributed Energy Supply System Based on Solar and Biomass Energy. *Acta Energetica Solaris Sin.* **2019**, *40*, 3164–3171.
22. Cui, H.; Zhang, L.; Ma, K.; Zhang, X. Research on the Combined Heating System of Solar, Biomass, and Valley Electricity Thermal Storage. *Hebei J. Ind. Sci. Technol.* **2022**, *39*, 439–448.
23. Zhang, M. Analysis of Solar Heating Energy Consumption in Kunming Area during Winter. Master's Thesis, Yunnan Normal University, Kunming, China, 2022. (In Chinese with English Abstract). [\[CrossRef\]](#)
24. Zhang, I. Simulation Study on the Performance of the Solar Air Source Heat Pump Dual Water Tank Composite Heating System in Rural Beijing. Ph.D. Thesis, Beijing University of Civil Engineering and Architecture, Beijing, China, 2020. [\[CrossRef\]](#)
25. Caliskan, H. Thermodynamic and Environmental Analyses of Biomass, Solar, and Electrical Energy Options for Building Heating Applications. *Renew. Sustain. Energy Rev.* **2015**, *43*, 1016–1034. [\[CrossRef\]](#)
26. GB/T 51366-2019; Standard for Calculation of Building Carbon Emissions. China Building Industry Press: Beijing, China, 2019.

**Disclaimer/Publisher's Note:** The statements, opinions and data contained in all publications are solely those of the individual author(s) and contributor(s) and not of MDPI and/or the editor(s). MDPI and/or the editor(s) disclaim responsibility for any injury to people or property resulting from any ideas, methods, instructions or products referred to in the content.